ELSEVIER

Thermochimica Acta 391 (2002) 51–67

thermochimica acta

www.elsevier.com/locate/tca

Calibration of magnitude and phase angle of TMDSC Part1: basic considerations

G.W.H. Höhne[a], M. Merzlyakov[b,1], C. Schick[b,*]

[a]*Dutch Polymer Institute, Eindhoven University of Technology, P.O. Box 513, 5600 MB Eindhoven, The Netherlands*
[b]*University of Rostock, FB Physik, Universitätsplatz 3, 18051 Rostock, Germany*

Received 29 September 2001; received in revised form 29 January 2002; accepted 31 January 2002

Abstract

The basic principle of heat transfer in temperature-modulated differential scanning calorimetry (TMDSC) and its influence on the measured signals is presented. Fundamentals of transfer theory are given within the framework of linear response. On this basis different calibration methods are suggested which enable to correct for the influence of heat transfer on the measured (effective) complex heat capacity in TMDSC. It is shown, that the complex calibration function is the reciprocal transfer function, which in turn is the product of the instrumental transfer function and the transfer function of the sample and its thermal connection to the TMDSC. Methods are given how to determine the transfer functions and how to correct the measured complex heat capacity properly.

Keywords: TMDSC; Calibration; Complex heat capacity; Heat transfer; Correction

1. Introduction

Temperature-modulated differential scanning calorimetry (TMDSC) is nowadays widely used to investigate time dependent processes as well as to determine the heat capacity of materials. This is done by calculating the interesting quantities from magnitude and phase angle (relative to that of the modulated temperature function) of the measured heat flow rate. Unfortunately the measured quantities contain influences from the apparatus (the DSC) too and careful ''calibration'' should be done to separate these influences from the measured signal and come to reliable results of the properties of the sample itself. Calibration means the quantitative determination of all apparatus influences and the proper correction of the measured raw data. In common DSC the calibration procedures for temperature, heat flow rate and heat are well established in practice [1] and for commercial DSC normally part of the software. For TMDSC there is an additional calibration procedure needed which corrects for the huge influence of the frequency on the magnitude and phase angle of the measured complex heat capacity.

This paper aim at making a contribution to better understand the influence of the TMDSC on the measured complex heat capacity and to give a procedure to determine the falsification quantitatively and correct it. At first we present the TMDSC and the pathway of

* Corresponding author. Tel.: +49-381-498-1644; fax: +49-381-498-1626.
E-mail address: christoph.schick@physik.uni-rostock.de (C. Schick).
[1] Present address: Chemical Engineering, P.O. Box 43121, Texas Tech University, Lubbock, TX 79409, USA.

0040-6031/02/$ – see front matter
PII: S0040-6031(02)00163-6

heat transfer by means of very simple model considerations leading to some formulas describing this behavior approximately. These considerations form the basis for different calibration procedures for the magnitude as well as the phase angle of the complex heat capacity of the sample, which we present in Section 3 of this paper. The aim is to give the practician a method which enables him to measure accurate complex heat capacities (i.e. magnitude and phase angle or real and imaginary part) with commercial DSC in temperature-modulated mode. We shall do that in different steps starting from rather simple calibration methods (in part already published by other authors) and proceeding to more complex methods which need more effort but enables the interested and more advanced user to come to better results. To understand these procedures better, it would of course be helpful to study the basic model considerations in Section 2 of this paper first, but it is even possible to refrain from understanding the background and simply make use of the recommended methods. In a second part [2], we shall demonstrate the capabilities and limits of the different methods applying the methods described to one set of experimental data from a model substance.

2. Components of a DSC model

A DSC is built from different parts, which in principal have a certain heat conductivity and a certain heat capacity each. Any contact area between different parts acts as an additional heat resistance. In addition it includes often some sophisticated electronics that amplifies the voltages from the sensors to the measured signal transferred to the computer. This way a DSC, no matter how complicated it is, can be dissected into a network of simple mechanical elements and the, hopefully, linear electronics. There is no limit for the number of elements in such a network. To get the properties of it, a system of linear differential equations must be solved. The number equals the number of elements in question, this number can be high for complex modern equipment, but, thanks to modern computers and adequate mathematics software, the solution is in principle possible. Nevertheless we shall, in what follows, restrict ourselves to very simple models, which are absolutely sufficient for to learn about the principle behind heat transfer in the DSC and to the sample and its influence on TMDSC signals.

The model of choice to evaluate a heat transfer network is often that of electrical analogy, which has proved its worth in DTA and DSC analysis since decades [3]. From the physical point of view the transport of energy (heat flow) is based on the same type of equations, as is the transport of charge (current), so the knowledge from theory of electricity (in particular alternating current (ac) theory) can easily be transferred to heat transport problems. The advantage of looking on electrical networks rather than on often complex heat conducting solid objects is that there are a lots of powerful tools from electrical line network as well as transfer theory available for our purpose and the ''wheel'' has not to be invented once again.

The total network describing a DSC (the ''box'') has one ''input'' (the temperature-time program) and one ''output'' (the heat flow rate into the sample, which is calculated from the differential temperature or directly measured as differential heat flow rate). To evaluate the behavior of an apparatus it is often sufficient to look at the so-called ''transfer function'' $P(\omega)$ of the ''box'', a complex function in frequency domain [4,5], which is defined as the quotient of the output function $\mathrm{Out}(\omega)$ over the input function $\mathrm{In}(\omega)$. The transfer function (in frequency domain) is mathematically connected with the ''step response'' or ''pulse response'' functions (in time domain) via Fourier transform. It will go beyond the scope of this paper to derive all details of the features of these functions; the interested reader is referred to textbooks of transfer theory. However, the transfer function of the apparatus is in principle the ''calibration'' function we need to correct the measured quantities for apparatus influences.

From transfer theory of linear systems, it is known that the overall transfer function of a network can be calculated from the transfer functions of the individual components [4,5]. In particular it holds that for transfer elements connected in series the total transfer function is the product of those from the elements. In other words, the magnitudes of the complex functions must be multiplied, whereas the phase angles connect additively. On the other hand, for transfer elements connected in parallel the total transfer function is the sum of those of the components.

These facts enable to breakdown the rather complicated heat transfer network of a DSC into simple components with rather simple transfer functions (for reasons of understanding the principle behind). These transfer functions can then be assembled properly and give the transfer behavior of the total TMDSC (both with and without the sample included). We shall proceed this way in this paper and look at the single components first and connect the results later. Knowing the transfer function enables the determination of the correction function and thus a proper calibration.

2.1. The RC-element

The simplest component of heat conducting networks is an object having a certain thermal resistance R_{th} and a certain heat capacity C_p. The respective electrical analogy element is the low-pass filter built of a resistor R and a capacitor C. The complex transfer function, taking ac-voltage as input and output functions, can easily be calculated, it is:

$$P(\omega) = \frac{1}{1 - i\omega RC} = \frac{1}{1 + (\omega RC)^2} + \frac{\omega RC}{1 + (\omega RC)^2}\, i \tag{1}$$

with the angular frequency $\omega = 2\pi f$ (f frequency). Changing R to R_{th}, C to C_p and voltage to temperature gets the respective transfer function for the thermal behavior of such an element. Thus, we calculate the magnitude (absolute value, modulus):

$$\mathrm{Abs}(P(\omega)) = \sqrt{\mathrm{Re}^2(P) + \mathrm{Im}^2(P)} = \frac{1}{\sqrt{1 + (\omega R_{th} C_p)^2}} \tag{2}$$

and the phase angle (argument):

$$\mathrm{Arg}(P(\omega)) = \tan^{-1}\left(\frac{\mathrm{Im}(P)}{\mathrm{Re}(P)}\right) = \tan^{-1}(\omega R_{th} C_p) \tag{3}$$

of the complex transfer function in the case of thermal quantities. From these equations follows that the magnitude of the (modulated) temperature on the output side (compared to the input side) drops with increasing frequency and there is a phase shift between both signals. With other words the measured quantities (output) are not constant for a constant input function but depend on the frequency in question. The change (falsification) of the output quantities is the larger, the larger the frequency of temperature modulation, the heat capacity and the thermal resistance of the considered *RC*-element.

For a given heat conducting element with given R_{th} and given C_p (the product is a characteristic time τ), the frequency dependence of the complex transfer function can be presented graphically in different ways. One method is to plot the logarithm of magnitude (2) and the phase angle (3) separately (in log scale: "Bode plot", Fig. 1). Another way is to plot the imaginary part (1) against the real part (1) in a polar diagram in the complex plane with the frequency as an implicit parameter ("Cole–Cole plot", Fig. 2). However, we prefer the first method because it seems to be easier to handle and to interpret.

The log–log plot of the magnitude of the transfer function (Fig. 1 upper curve) of the simple *RC*-element discussed shows some characteristics; for low as well as for high frequencies this function becomes a straight line (asymptotes with slopes of 0 and -1, respectively) which intersect at a certain frequency ω_0, the "corner frequency" of the *RC*-element. The phase angle (Fig. 1 lower curve) at ω_0 is just half ($\pi/4$) of its total value ($\pi/2$). The corner frequency is reciprocally connected with the characteristic time of the *RC*-element: $1/\omega_0 = \tau = R_{th} C_p$.

To calculate the (complex) heat flow rate into a *RC*-element from the transfer function (1) for a given modulated temperature function (with frequency ω), we have to multiply it with C_p and ω. The magnitude of that function is got easily in the Bode plot via a simple shift in y-direction of the magnitude of the transfer function (Fig. 1), which leaves the shape of the curve unchanged. To get the phase angle of the heat flow rate, we have to take a phase jump of $\pi/2$ between temperature and heat flow into consideration, which we have to subtract from the argument of the transfer function. Again this is a simple shift in y-direction in the Bode plot (Fig. 1) leaving the shape of the curve unchanged. Here the advantage of the Bode plot becomes obvious the first time. The calculation of the real heat flow rate (magnitude and phase angle) is very simple. To get the proper heat flow (or C_p) curve of a certain *RC*-element, we only have to shift the transfer function properly in the Bode plot.

It should be noticed that the sample (including crucible) normally behaves like a simple *RC*-element

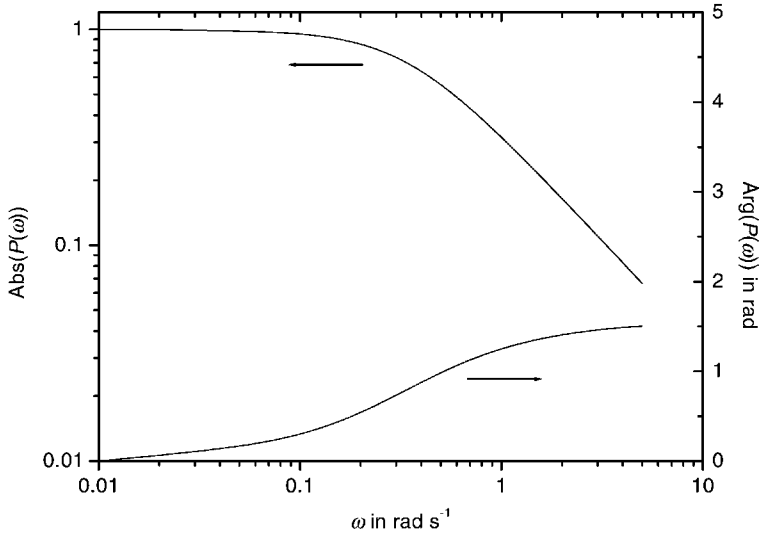

Fig. 1. Bode plot: magnitude (upper) and phase angle (lower) of transfer function of an *RC*-element ($R_{th} = 0.03$ K mW^{-1}, $C_p = 100$ mJ K^{-1}, $\tau = 3$ s).

in a TMDSC which is shown in what follows. In Fig. 3, the measured transfer functions (i.e. the normalized measured heat capacity) of four aluminum discs in a PerkinElmer instruments Pyris-1 DSC is given. Because of the high thermal conductivity of aluminum, it is clear that these samples should behave like a simple *RC*-model composed of the total heat capacity (sample + pan) and the thermal resistance of heat transfer. But if we compare the results from Fig. 3 (especially the phase angle shift in Fig. 3b) with Fig. 1, it is obvious that the data cannot be described by a single *RC*-element. This is mainly caused by the transfer function of the instrument itself, which is included in the results of Fig. 3. After subtraction of the proper transfer function of the instrument the behavior of all four samples is well described by a

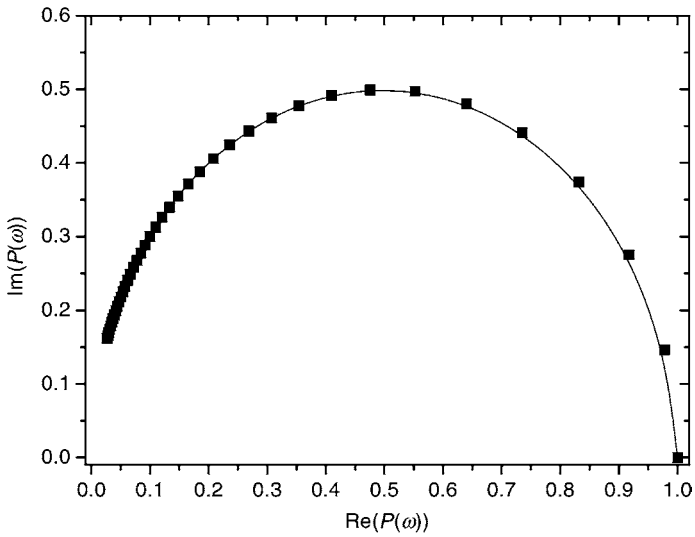

Fig. 2. Cole–Cole plot of the transfer function of an *RC*-element with ω as parameter ($R_{th} = 0.03$ K mW^{-1}, $C_p = 100$ mJ K^{-1}, $\tau = 3$ s).

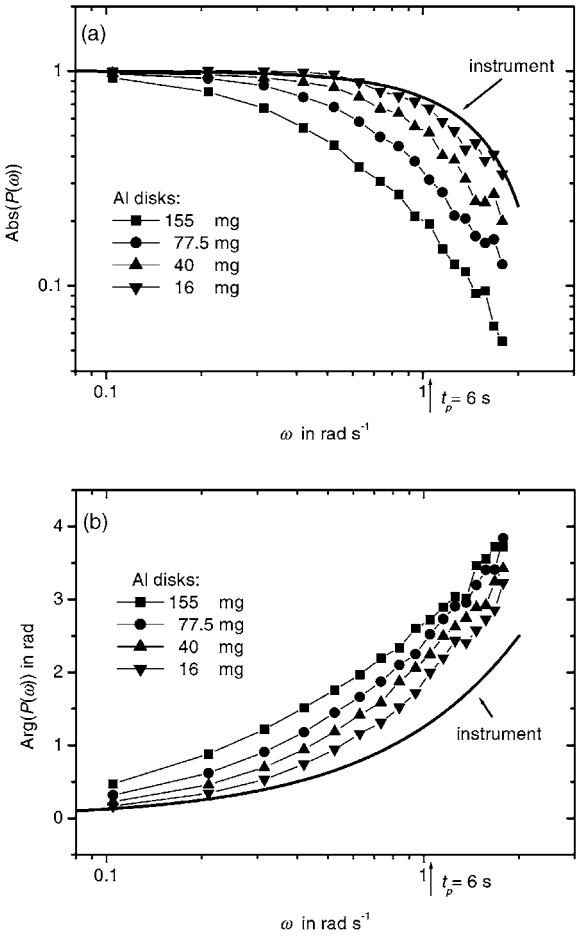

Fig. 3. Bode plot: magnitude (a) and phase angle (b) of the total transfer function of a PerkinElmer Instruments Pyris-1 DSC with different Al discs (symbols) together with the transfer function of the empty instrument (solid line, see Section 3.4).

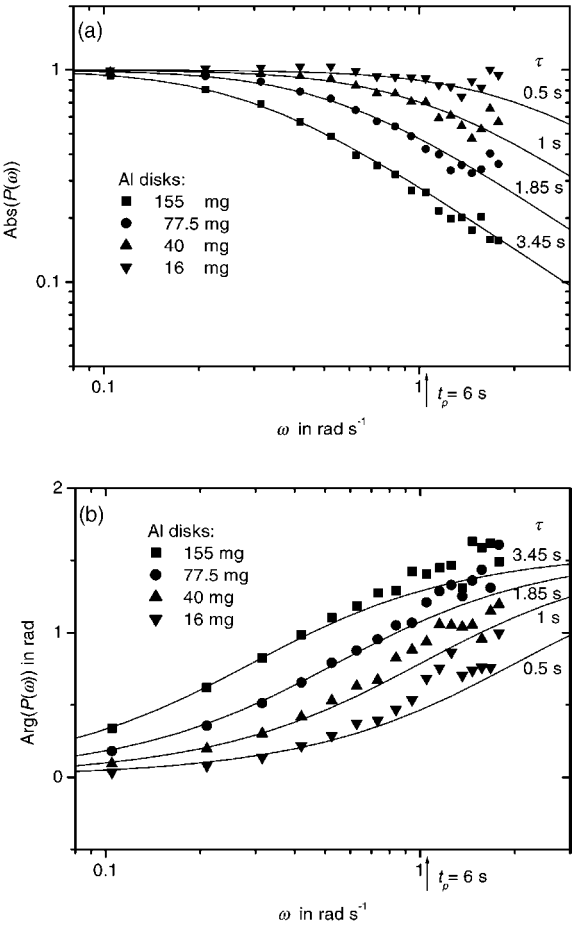

Fig. 4. Bode plot: magnitude (a) and phase angle (b) of the sample part of the transfer function from Fig. 3 (symbols) together with the fit function using Eqs. (2) and (3), respectively (solid lines). From the fit parameter τ, an effective thermal resistance can be determined: $R_{th} = 23\ K\ W^{-1}$. PerkinElmer Instruments Pyris-1 DSC.

simple *RC*-element composed of the heat capacity in question and an almost constant thermal resistance as shown in Fig. 4. In what follows we shall discuss the reasons for the additional contributions to the total transfer function and how to obtain them.

2.2. RC-element networks

The simple *RC*-element can even be helpful to model the properties of the total equipment, i.e. the apparatus (DSC) plus sample what concerns the heat transport influence on the measurement. In a first approximation the heat flows along an one-dimensional pathway through the DSC. This can be modeled by a series of *RC*-elements. The simplest model contains three elements: one, for instance, for the part of the pathway from the oven to the thermometer, one from the thermometer to the sample (or reference) support (or pan) and one from there to the inner of the sample (or reference). All these *RC*-elements have different (apparent) heat resistances and different (apparent) heat capacities, which, of course, are unknown for the user but almost fixed concerning the apparatus part (but they differ for the sample part). If needed these data can be determined from the measured transfer function as will be shown elsewhere.

From transfer theory it is known, that for transfer elements connected in series the total transfer function is the product of the transfer functions from the elements. In other words, the magnitudes (amplitudes) have to be multiplied, whereas the phase angles connect additive. This way the total transfer function can be deduced from Eqs. (1)–(3) with different $\tau_j = R_{\mathrm{th},j}C_{p,j}$ for the different *RC*-elements in question:

$$\mathrm{Abs}(P(\omega)) = \prod_j \frac{1}{\sqrt{1 + (\omega R_{\mathrm{th},j}C_{p,j})^2}} \quad \text{and}$$

$$\mathrm{Arg}(P(\omega)) = \sum_j \tan^{-1}(\omega R_{\mathrm{th},j}C_{p,j}) \tag{4}$$

From the multiplicative behavior of the magnitude another advantage of the Bode plot becomes obvious: the slope of the high frequency asymptote in the log–log plot characterizes the number of effective different *RC*-elements involved. One *RC*-element will give a slope of -1 (Fig. 1); two *RC*-elements in series will give a slope of -2 and so on.

It should be mentioned too, that for transfer elements connected in parallel the total transfer function is the sum of the transfer functions of the respective elements:

$$P(\omega) = \sum_j P_j(\omega) \tag{5}$$

2.3. A simple DSC model

As an example for modeling a DSC, the simplest possible network is as follows (Fig. 5): One *RC*-element on the reference side, $R_{\mathrm{th},1}$; $C_{p,1}$, (collecting the heat flow path and the pan together) and two *RC*-elements in series on the sample side, $R_{\mathrm{th},1}$; $C_{p,1}$; $R_{\mathrm{th,s}}$; $C_{p,\mathrm{s}}$ (the apparatus part and the sample separated).

The transfer function for this model is again defined as the quotient of the output function (i.e. the ΔT signal of the DSC) over the input function (i.e. the temperature of the heater T_{fur}). It can be calculated straight forward in analogy to the single *RC*-element, see [6–8]:

$$P(\omega) = \frac{\Delta T}{T_{\mathrm{fur}}} = \frac{1}{1 - i\omega R_{\mathrm{th},1}C_{p,1}} - \frac{1}{1 - i\omega R_{\mathrm{th},1}C_{p,1} + ((R_{\mathrm{th},1}/R_{\mathrm{th,s}} - (1/i\omega C_{p,\mathrm{s}}))} \tag{6}$$

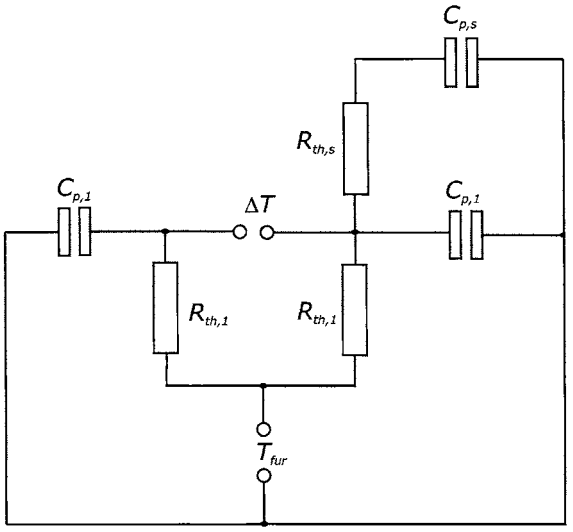

Fig. 5. Circuit representing the simplest model for a DSC, see text.

This is simply the difference of the transfer functions of a single low pass and that of two low passes in series, representing the reference side and the sample side of a differential calorimeter, respectively. The quantities $R_{\mathrm{th},1}$ and $C_{p,1}$ characterize the (apparent) thermal resistance and the (apparent) heat capacity of the heat flow pathway from the furnace to the inner side of the pans, which are thought to be identical on sample and reference side. $R_{\mathrm{th,s}}$ and $C_{p,\mathrm{s}}$ symbolize similar quantities for the sample itself (Fig. 5). The magnitude and phase angle of the complex transfer function (6) was calculated using MAPLE mathematics software and plotted in Fig. 6 (solid lines) after inserting reliable values for the parameters. The curves look similar to the curves in Fig. 1, but the slope of the asymptote at higher frequencies is about -2 in this case and the phase angle shift is much larger, nevertheless the model describes the behavior of a real DSC (see measured values in Fig. 6) only approximately.

The model can be refined with additional *RC*-elements both on the reference and on the sample side. In a second approximation, we may use two serial *RC*-elements on the reference side and three on the sample side, characterizing the heat path between the heater and the temperature sensor, between the thermometer and the inner side of the pan and the sample itself, respectively. The transfer function of this network,

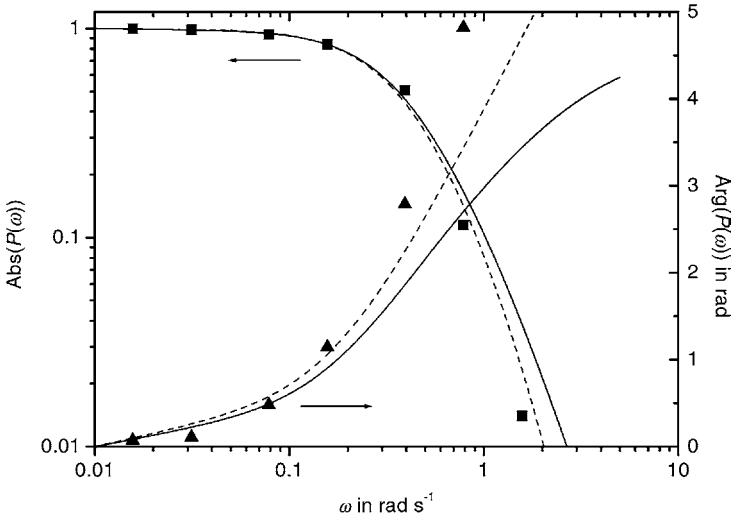

Fig. 6. Bode plot: magnitude (upper) and phase angle (lower) of transfer functions of different DSC models; solid lines: the model of Eq. (6) with $R_{th,1} = 0.02$ K mW^{-1}, $C_{p,1} = 130$ mJ K^{-1}, $\tau_1 = 2.6$ s, $R_{th,s} = 0.1$ K mW^{-1}, $C_{p,s} = 6.5$ mJ K^{-1}, $\tau_s = 0.65$ s; dotted lines: more detailed model with $R_{th,1} = 0.02$ K mW^{-1}, $C_{p,1} = 100$ mJ K^{-1}, $\tau_1 = 2.0$ s, $R_{th,2} = 0.03$ K mW^{-1}, $C_{p,2} = 20$ mJ K^{-1}, $\tau_2 = 0.6$ s, $R_{th,s} = 0.1$ K mW^{-1}, $C_{p,s} = 6.5$ mJ K^{-1}, $\tau_s = 0.65$ s; symbols: measured values of $C_{p\ \mathrm{measured}}/C_{p\ \mathrm{true}}$ (squares) and phase angle (triangles) of a 20 mg sapphire disc in a PerkinElmer Instruments DSC-7.

which can be deduced straightforward, is presented in Fig. 6 (dotted lines) using a reliable set of values for the different resistances and capacities. The overall shapes of these functions are again not very different from those of the simpler model (solid lines) though the exact formula is much more complicated and contains much more parameters. The reason why we present it here is to show, that the magnitude curve is not changed very much (it is somewhat steeper again), whereas the phase angle is much more sensitive to model changes. In principle the model can be extended even further by adding more and more *RC*-elements, such examples can be found in literature [7,9–12], but the question arises whether this is really helpful way to get the true calibration function for the TMDSC in question. With increasing number of *RC*-elements in the model the number of parameters increases as well and in principal every real TMDSC can be described this way, but the problem remains how to obtain the correct values for the increasing number of parameters. Furthermore the question arises whether the certainty of the results is really improved by using an only approximate model with a lot of parameters which have to be determined with additional measurements. Another argument is, that modern equipment often contains other elements which possibly cannot be described with a simple *RC*-network.

2.4. Electronics and data processing

Every DSC nowadays contains electronic controllers and amplifiers for signal processing and the question arises how they may influence the measured signal. The answer is easy in the case of modern analog (dc) amplifiers, they contain operational amplifiers and other linear components only and the bandwidth is so large (kHz) that there is no influence on the signal of common TMDSC. The situation is different, however, if electronically signal smoothing is used to improve the signal-to-noise. Here we have to distinguish between passive and active filtering. The former is normally done with an electronic low pass filter (i.e. a *RC*-element), which already has been presented in Section 2.1 (Eq. (1)). If such a filter is included in the electronics of the DSC, we have to add one more serial *RC*-element into the network model, in other words the transfer functions of the DSC and that of the filter in question have to be multiplied (i.e. addition of the respective Bode plots) to get the total transfer function.

If active filtering is performed (by hard- or software) the influence on the signal cannot be determined without further knowledge about the method used. Unfortunately this information is often confidential and not easy to get, but nevertheless it is essential for the behavior of the equipment, in particular as there are even non-linear methods used in practice. This is a dilemma and there is no other way out than to test the apparatus experimentally, e.g. with the methods presented in Section 3.

Another type of amplifier (often used for amplification of very weak signals) is the chopper-amplifier. With this technique the signal (e.g. that from the ΔT sensor) is periodically grounded resulting in a periodical signal, which then is processed using more sensitive ac-amplification techniques. However, the effect of the chopper on the transfer function of such an amplifier is similar to the influence of a low-pass filter (Section 2.1) with the chopper frequency acting as corner frequency. Normally the chopper frequency (50 Hz or more) is much higher than the frequency range of the TMDSC and there is no measurable influence on the signal. But there may be an interference of the chopper frequency with the line frequency of 50 (60) Hz and the differential frequency could fall into the frequency window of the temperature modulation and this way influence the measured signal.

Every DSC contains (electronic) controllers for temperature control and—if existent—power compensation. Normally such controllers work linearly using the PID principle (a Proportional amplifier, an Integrator and a Differentiator normally in parallel). The transfer function of the P-element is simply a constant factor. The I-element is identical to a low-pass filter (Eq. (1), Fig. 1). The D-element, in turn, behaves like a high pass filter and its transfer function is like that of a low-pass filter (Fig. 1) but mirrored at the $y = 1$ axis (i.e. the slopes of the asymptotes are in this case 0 and $+1$, respectively). For the PID, all three elements are connected in parallel and act on the temperature of the heater, which is the input quantity of our model. This means, that the sum of the respective transfer functions (i.e. the total PID) acts multiplicative on the transfer function of the DSC evaluated in Section 2.3 (i.e. the respective Bode plot has to be added).

There is, however, another effect with control circuits that has an essential influence on the transfer behavior. This is a certain time lag (''dead-time'' τ_d) between an action of the controller and the reaction of the controlled element (heater), which is caused by the inertia of the controlled path. If such a dead-time exist, there is an additional phase angle shift

$$\varphi_d = \tau_d \omega \tag{7}$$

whereas the magnitude of the transfer function remains unchanged.

Of course, even the sampling rate of the analog–digital converter, involved in nowadays data processing is a limiting factor. Let Δt_c be the time interval between data points in time domain, then it follows from Fourier transform that every (even non-periodic) sampled function becomes periodical in frequency domain with a period:

$$\Delta_p \omega = \frac{1}{\Delta t_c} \tag{8}$$

This periodicity is an artifact caused by the sampling, which falsifies the true function in frequency domain and in the same moment limits the frequency range of that function. As a rule of thumb, the sampling interval should be chosen at least 20 times smaller than the period of the modulation to get reliable results (i.e. falsification <5%) for the Fourier transformed signal.

2.5. Thermal waves

Another approach to describe the behavior of poor heat conducting materials (e.g. polymer samples) in a TMDSC starts from the (one dimensional) heat diffusion equation:

$$\frac{\partial T}{\partial t} = D_{th} \frac{\partial^2 T}{\partial x^2} \tag{9}$$

with D_{th} the thermal diffusivity. From this equation follows, that a temperature change at the border of a conductor proceeds through it as a damped thermal wave. In this case, we have to consider the sample as an infinite series of infinitesimal small *RC*-elements rather than a series of some *RC*-elements used for the simple formula (4) which leads to wrong results, if the sample is so big, that a damping of the thermal wave (i.e. change of the temperature amplitude) inside the sample becomes significant. In this case the proper solution of the diffusion Eq. (9) must be used

which depends on the particular boundary conditions. Examples can be found in literature [13–20].

2.6. Conclusions concerning the behavior of the TMDSC

The reason for the relative broad presentation of the transfer behavior of the TMDSC was to enable the experimenter to get better insight about the influence of heat transfer on the measured quantities. Up to now, in all our considerations a linear behavior of the DSC (and all its components including data processing) was assumed. Unfortunately, there are other effects that disturb the measurements and may lead to faulty results. There can be a possible non-linearity which often is not obvious for the experimenter. One fact is that any asymmetry between the sample and reference side in the DSC result in problems, in particular when not reproducible, this should be detected and, if possible, eliminated. To prove the linearity and find possible exceptions from it, we are in need of a proper experimental procedure. We are as well in need of a method to get the proper calibration function to calculate the true magnitude and phase angle of the (complex) sample heat capacity from the measured raw data. The mentioned transfer function can be helpful in this case.

If we compare the calculated transfer function for different DSC models with that from real measurements of a sapphire sample at different frequencies (Fig. 6), it becomes obvious that these rather simple models describe a real TMDSC rather well. The improved network model with three *RC*-elements on the sample side and two on the reference side is better than the simpler one. The magnitude fits better to the measured values than the phase angle does, the phase angle seems to be more sensitive to the model in question. However, these models are approximations for the heat transfer behavior only, the possible influences of electronics and control circuits are not included and can hardly be included exactly because of missing knowledge of the details which may differ for the different DSCs.

To summarize the results we can state, that the real DSC used in the TMDSC mode behaves like the simple models presented above. The (reciprocal) transfer function calculated with proper parameters may serve as calibration function to correct the measured raw data for frequency influences. The magnitude (in particular the static heat capacity of the sample) is rather well corrected this way, whereas the phase angle correction, necessary to get the correct complex heat capacity of the sample, is rather uncertain. Consequently we are in need of a suitable method to determine the real transfer function experimentally, which then can be used to calibrate the magnitude and the phase angle of the measured signal and correct for apparatus influences. We shall present different calibration procedures in what follows.

3. Calibration procedures

In this section, we want to give the practician a calibration method into the hand which enables him to measure exact complex heat capacities with commercial DSC in the temperature-modulated mode. To begin with, we would like to summarize the considerations which the calibration methods are based on.

The TMDSC is a linear device, and the behavior concerning the heat conduction can be described quantitatively with the tools of transfer theory. This can be done in time domain using either the pulse response (Greens) or the step response function, or in frequency domain using the complex transfer function (i.e. the normalized quotient of the output over the input function). All three functions are equivalent and can be converted into one another mathematically by integration, differentiation and Fourier transform, respectively.

Linear response implies the possibility to breakdown a complex device into a network of simple elements with known transfer behavior. For serial connection of elements the total transfer function is the product of the single transfer functions. For parallel connection, the total transfer function is the sum of the single transfer functions. In the case of TMDSC, the apparatus and the sample can be considered as connected in series, in other words the total transfer function is the product of the transfer function of the DSC itself and the transfer function of the sample. The simplest component is a *RC*-element with a certain thermal resistance R_{th} and a certain heat capacity C_p, this is in general a suitable model for a (not too big) sample and its thermal connection to the DSC. For the (complex) transfer function of the *RC*-element see Eqs. (1)–(3).

Because of the thermal behavior, the effective heat capacity of a sample, measured in a TMDSC, depends always on frequency. To get the correct heat capacity, we have to divide the measured heat capacity (at a certain frequency) with the value at that frequency of the transfer function of the TMDSC used. In case of "multi-frequency" TMDSC measurements, we get the effective complex heat capacity not only at one frequency but as a series of values at the base frequency and its higher harmonics or as a continuous function $C_{p,\text{meas.}}(\omega)$ which should be divided by the transfer function to get the correct complex heat capacity of the sample.

Division of complex functions means division of the (real valued) magnitudes and subtraction of the phase angles (i.e. the respective Bode plots of the complex functions have to be subtracted). Thus, we get the corrected heat capacity:

$$C^*_{p,\text{corr.}}(\omega) = \frac{C^*_{p,\text{meas.}}(\omega)}{P(\omega)} \tag{10}$$

and with the well-known relation for a complex quantity $C^*_{\text{p}}(\omega) = C_{\text{p}}(\omega)\,\text{e}^{i\varphi}$, we find:

$$C_{p,\text{corr.}}(\omega) = \frac{C_{p,\text{meas.}}(\omega)}{\text{Abs}(P(\omega))} \quad \text{and}$$
$$\varphi_{\text{corr.}} = \varphi_{\text{meas.}} - \text{Arg}(P(\omega)) \tag{11}$$

for the magnitude (absolute value) and the phase angle shift, respectively.

Calibration means to determine the transfer function of the TMDSC in question including the sample and to correct the measured effective heat capacity properly. The calibration function for this correction is identical with the reciprocal transfer function of the apparatus (including the control and evaluation hard- and software).

The TMDSC method allows to measure the (real valued) static heat capacity as well as the complex heat capacity in case of (time dependent) dynamic processes. For many applications, it is sufficient to measure only the absolute value of the apparent heat capacity and disregard the phase angle, that is why we firstly describe the calibration of the magnitude only and proceed to the more complete calibration of the complex heat capacity later.

Some general remarks concerning the TMDSC measurements should be included:

We recommend to perform zeroline correction generally for TMDSC measurements to exclude the influence of possible asymmetry of the DSC instrument. Simple subtraction of the zeroline heat flow (got with empty pans of same type and mass) from the sample heat flow in time domain before evaluation is sufficient in most cases. Zeroline correction can appreciably improve the accuracy of the measurements as long as the temperature time profile is the same for both measurements.

One should even bear in mind that software filtering, used sometimes to reduce the noise-level, leads to additional "smearing" of the heat flow signal and changes the transfer function distinctly.

With this background, we can start to discuss the calibration methods in what follows.

3.1. Simple heat capacity calibration

This method corresponds to the common heat flow rate calibration of standard DSC which uses the known heat capacity of reference materials (as sapphire) to calibrate the calorimeter. In principle this well-known procedure could even be used with TMDSC, but, as the temperature-modulated measurements are very sensitive to the heat transfer conditions to the sample and the heat conductivity within the sample itself, this method may give incorrect results, because the heat conductivity of the normally used reference material (sapphire) is in principle different from the heat conductivity of the sample (e.g. a polymer). The resulting error is larger the difference and larger the frequency of the temperature modulation used. This way the advantage of the very precise heat capacity values of the reference materials is lost and we can refrain from this calibration method and come to a simpler one.

Often the (static) heat capacity of the sample material itself is known, or can be found in literature, and we can use this knowledge for an in situ calibration. The procedure is easy: we have to measure the heat capacity with the TMDSC at a certain frequency in a temperature region well outside of any transition or reaction of the sample and compare the result with the literature value. This yields a correction factor for the frequency (and temperature) in question which enables a proper calibration. This method can be used in scanning as well as in quasi-isothermal mode. If the temperature dependence of the heat capacity of the

sample is known we can get the calibration function (for that frequency) in dependence of temperature too. The method is already widely used in TMDSC because of the simple straight forward handling. The accuracy is determined by the accuracy of the TMDSC evaluation and, of course, the accuracy of the literature values of the heat capacity of the sample.

Although often disregarded this method allows a simple phase angle calibration too; outside a transition region, where the heat capacity is real valued, the phase angle should be zero. This makes a simple correction for the phase angle possible, namely to connect the measured phase angle outside the transition properly and subtract this ''phase angle-baseline'' from the measured phase angle.

It should be mentioned, that this simple method may give wrong results, as the thermal resistance often changes in a unknown manner during transitions (e.g. glass transition or melting), this would lead to a correction factor which is different before and after a transition and, in addition, may not change linearly during the transition. Furthermore, the sample heat capacity may change considerably during a transition, which together with a change of the thermal resistance result in an often huge change of the transfer function (and with it the calibration function) during transitions. This means, that a simply interpolated correction would give a wrong calibration in the region of such transitions.

3.2. Calibration procedure from multi-frequency evaluation

Using sawtooth-type or multi-step temperature modulation with TMDSC enables multi-frequency evaluation of heat capacity from one single scanning or quasi-isothermal run. Recently Wunderlich and coworkers [21,22] have presented a calibration procedure, which uses the advantages of this evaluation method to get the correct magnitude of the heat capacity. The idea is to determine the heat capacity for different frequencies (the higher harmonics of the basic period) and extrapolate to zero frequency (the standard case), for which the DSC is assumed to be calibrated in the normal manner. The authors present a formula for the heat capacity correction function:

$$K(\omega) = \sqrt{1 + \tau^2\omega^2} \tag{12}$$

which holds at least for lower frequencies [21]. This is exactly the reciprocal magnitude of the transfer function of a *RC*-element (Eq. (2)) with $\tau = R_{\text{th}}C_p$ which —for low frequencies—is a sufficient approximation, even for the TMDSC [8]. With the correction function (12), we get:

$$\frac{1}{C^2_{p,\text{meas.}}} = \frac{1}{C^2_{p,\text{corr.}}}(1 + (\tau\omega)^2) \tag{13}$$

Plotting the reciprocal squared measured heat capacity versus the squared angular frequency (Fig. 7) should result in a straight line with R^2_{th} the slope, and the corrected (squared) heat capacity the intercept with the ordinate at $\omega = 0$. This was proved to be correct for sapphire and polystyrene at frequencies up to $\omega = 0.4$ rad s^{-1} [22]. Of course the slope changes for different materials and different heat capacities, but this has no influence on the correction method itself, the intercept at $\omega = 0$ gives always the correct (static) heat capacity (if the DSC has been calibrated correctly in the standard mode). The method can even be used in cases, where the simple Eq. (12) doesn't hold. In such cases, the extrapolation is non-linear but comes to the correct value anyway. This procedure is very accurate and suitable for determination of common (static) heat capacities but can even be used for determination of the correct complex heat capacity if applied in a temperature region where no frequency dependent processes or transitions occur in the sample. Any correction of the phase angle is, however, not possible with this method. The remarks from Section 3.1 concerning the accuracy of the result and the interpolation in the region of transitions are valid as well in this case.

Recently Toda et al. [23] have published a calibration method (based on a DSC model of Hatta and Muramatsu [24]) which starts from a formula like that presented in Section 2.3. Determining the unknown parameters with a proper fit procedure the authors get an empirical correction function for the calibration which is more complex than Eq. (12).

3.3. Calibration using the step response function of the DSC

In this section, we present an easy method to determine the (complex) transfer function of the TMDSC including the heat transfer to the sample.

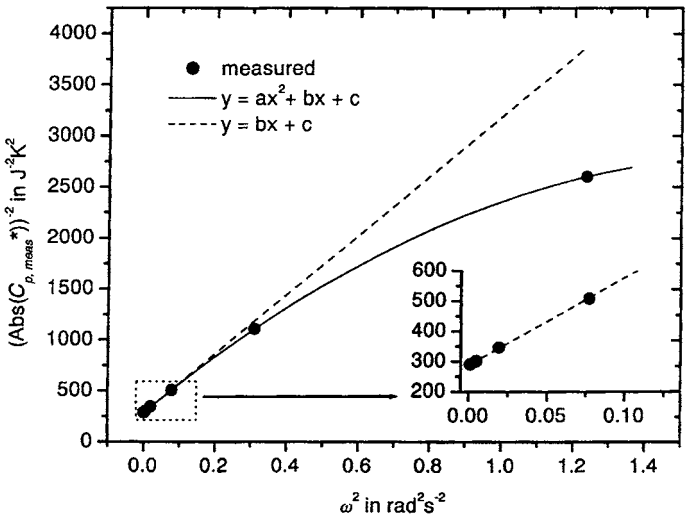

Fig. 7. Reciprocal squared measured heat capacity versus squared angular frequency for polystyrene, $m_s = 25$ mg, $T = 75$ °C. At frequency $\omega = 0.3$ rad s^{-1} ($\omega^2 = 0.09$ rad^2 s^{-2}) and lower measured points lie on a straight line. PerkinElmer Instruments Pyris-1 DSC.

Our method is based on the transfer theory, valid for linear behaving equipment, which tells us, that the transfer function is the Fourier transform of the pulse response function. The quantity measured in a DSC is the heat flow rate (HF, Fig. 8). A pulse in heat flow is equivalent to a step in temperature as "input function" of the DSC. The output function measured on a step-like temperature change is the searched pulse response function $P(t)$ of our TMDSC. This (normalized) function has to be Fourier transformed to yield the complex transfer function of the equipment:

$$P(\omega) = \mathrm{F}P(t) \tag{14}$$

Fourier transform—nowadays available in almost every data evaluation program as "fast Fourier transform"—normally yields the real and imaginary part of

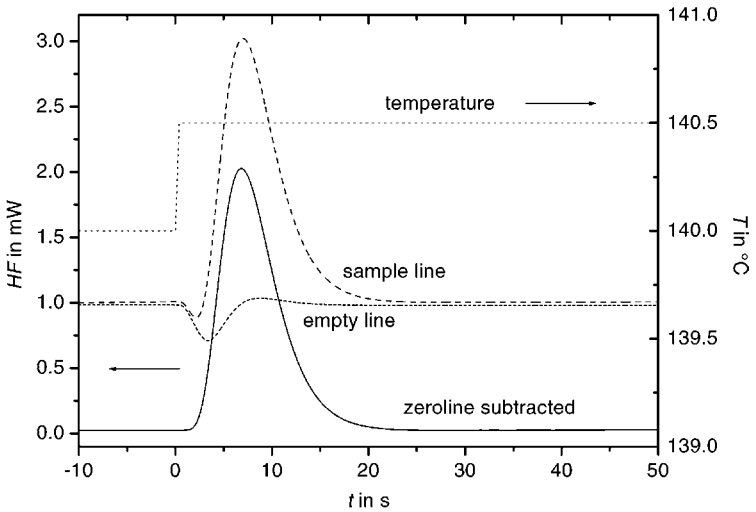

Fig. 8. Temperature step response function of a PerkinElmer Instruments DSC-7 containing a sapphire sample (25 mg).

the complex function. From these, one can easily calculate the magnitude and phase angle of the transfer function:

$$\mathrm{Abs}(P(\omega)) = \sqrt{\mathrm{Re}^2(P(\omega)) + \mathrm{Im}^2(P(\omega))} \quad \text{and}$$

$$\mathrm{Arg}(P(\omega)) = \tan^{-1}\frac{\mathrm{Im}(P(\omega))}{\mathrm{Re}(P(\omega))} \tag{15}$$

which are used then for correction of the measured apparent heat capacity by means of Eq. (11). The realization of this calibration method is as follows.

With the sample mounted, the DSC has to be programmed to a temperature where no transitions nor reactions occur in the sample. After equilibration, a temperature step of 0.5 K is programmed at maximum heating rate and the heat flow response is measured (time dependent) in isothermal mode. (Remark: the temperature step should be distinctly faster than the time constant of the DSC to give a correct result. If that, for certain DSCs, is not possible the more sophisticated method presented in Section 3.4 must be used for calibration.) The same procedure should be done with empty pans of same type and weight to get the zeroline which (as usual) must be subtracted from the sample curve to compensate for eventual asymmetries of the apparatus. The resulting differential curve is normalized and Fourier transformed yielding the transfer function $P(\omega)$, normalized as well (i.e. it is 1 for low frequencies). This function can be used then for correction of the measured apparent heat capacity with Eq. (11). To test the applicability of the method for a commercial DSC, we performed measurements of the apparent heat capacity (magnitude and phase angle) of a sapphire sample in quasi-isothermal mode at 140 °C at seven discrete frequencies. The magnitude was divided by the true heat capacity (Eq. (11)) and included in Fig. 9 (squares) together with the measured phase angle (triangles). Obviously the change of magnitude and phase angle of the heat capacity with frequency coincides with the transfer function (solid lines) calculated from the pulse response at 140 °C (Fig. 9). This supports the usability of this method and shows the accuracy of the correction as well. (To demonstrate the error one makes if the zeroline is not subtracted from the sample step response function before Fourier transform, such a curve has been added in Fig. 9 too).

Obviously, the step response method yields a more precise transfer function, than every DSC model does (compare Fig. 6), therefore it offers the possibility for a fast and simple heat capacity calibration method. It is of course possible to perform the step response method at different temperatures (before and after transitions) to test whether the transfer function and

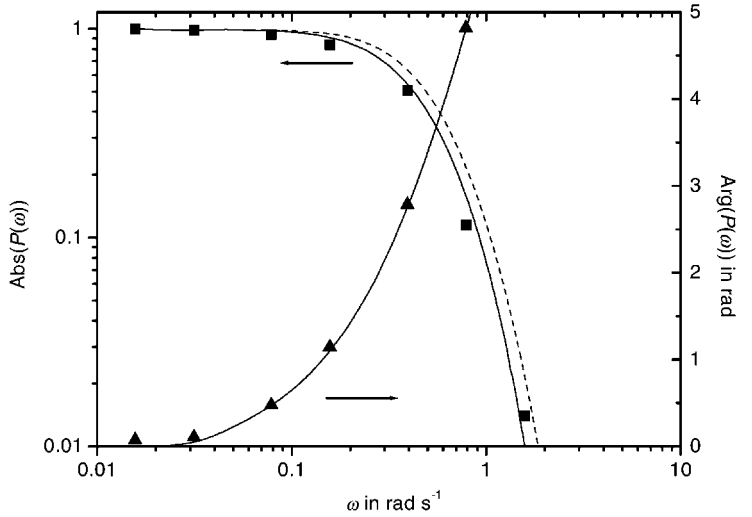

Fig. 9. Fourier transformed step response function from Fig. 8 (transfer function, solid lines) together with measured heat capacity (normalized to the value at zero frequency) of the same sample at different frequencies (symbols). The dashed line gives the magnitude of the transfer function from non zeroline corrected step response.

with it the calibration changes or not. It should be born in mind, that all remarks from Section 3.1 concerning the interpolation of the transfer or calibration function through a region of transition or reaction of the sample are still valid even with this method. Of course a correct heat flow calibration of the DSC in common scanning mode is a necessary prerequisite even with this method. Furthermore it should be emphasized, that this method yields the total transfer function including all heat transfer within the apparatus as well as to and within the sample, it therefore yields the correct calibration function even for thicker polymer samples, at least outside of transition regions. Different samples influence this total transfer function significantly, as can be seen in Fig. 3, all these influences are automatically covered using the step response method to get the calibration function.

3.4. Advanced calibration procedure

In what follows, we distinguish between the transfer behavior of the DSC instrument and that of the sample. The advantage is obvious, because the transfer behavior of the apparatus is normally the same for all measurements and it is sufficient to determine it once and use it for all further corrections. The sample part (heat transfer from the sample support to the pan and inside the sample) is, of course, different for every sample and the transfer function must be determined separately. As mentioned in Section 2 the total transfer function is the product of the apparatus part and the sample part, this means both parts are additive in the Bode plot. In Figs. 3 and 4, this is shown for Al-samples (discs) of different masses. Now the question arises how we can find the transfer function of the instrument itself (the thick solid line in Fig. 3).

For samples like a thin aluminum disc with high thermal conductivity one can neglect any temperature gradient inside the sample for frequencies relevant in TMDSC ($f < 1$ Hz). In such a case the sample itself can be considered as a simple *RC*-element (see Section 2.1) and the apparent (complex) heat capacity $C^*_\beta(\omega)$ of the sample (as it would be measured with an ideal TMDSC without thermal relaxation) at given frequency ω reads (see Eq. (1) and [25]):

$$C^*_\beta = \frac{C_p}{1 - (i\omega C_p / K_{\mathrm{op}})} \tag{16}$$

where C_p the (static) heat capacity of the sample disc and $K_{\mathrm{op}} = 1/R_{\mathrm{th}}$ the effective thermal contact between the sample and the heater (the thermal resistance of the sample itself is neglected). The measured (effective) heat capacity, which in frequency domain is calculated with:

$$C^*_{\mathrm{eff}}(\omega) \equiv \frac{\phi^*_{\mathrm{A}}(\omega)}{-i\omega T^*_{\mathrm{A}}(\omega)} = \frac{\phi^*_{\mathrm{A}}(\omega)}{\dot{T}^*_{\mathrm{A}}(\omega)} \tag{17}$$

($\phi^*_{\mathrm{A}}(\omega)$) complex heat flow amplitude, $T^*_{\mathrm{A}}(\omega)$ complex temperature amplitude, $\dot{T}^*_{\mathrm{A}}(\omega)$ complex heating rate amplitude, ω frequency) is normally different from the apparent heat capacity of the sample. The relation between both quantities can be expressed in the frequency domain, using a complex calibration factor, in the following form:

$$C^*_{\mathrm{eff}}(\omega) B^*_2(\omega) = C^*_\beta(\omega) \tag{18}$$

The dynamic (frequency depending) calibration factor $B^*_2(\omega)$ (for the reciprocal transfer function see Eq. (10)) includes all instrumental contributions (like thermal paths, feedback control circuits, filtering, software influences, etc.) which have an influence on the phase angle and the magnitude of the measured heat flow signals. We assume that $B^*_2(\omega)$ does not contain influences from the sample being measured. How can this function be determined?

Normally $C_\beta(\omega)$ of the sample disc with known heat capacity C_p is unknown because we do not know the actual value of the thermal contact K_{op} between the sample disc and the support. $B^*_2(\omega)$ can nevertheless be determined by measuring (at least) two different discs (say disc 'a' and 'b') in the following way.

Combining Eqs. (16) and (18) for disc 'a' yields:

$$C^*_{\beta,\mathrm{a}}(\omega) = C^*_{\mathrm{eff,a}}(\omega) B^*_2(\omega) = \frac{C_{p,\mathrm{a}}}{1 - (i\omega C_{p,\mathrm{a}} / K_{\mathrm{op,a}})} \quad \text{or}$$

$$B^*_2(\omega) = \frac{C_{p,\mathrm{a}} / C^*_{\mathrm{eff,a}}(\omega)}{1 - (i\omega C_{p,\mathrm{a}} / K_{\mathrm{op,a}})} \tag{19}$$

where $C^*_{\mathrm{eff,a}}(\omega)$ is measured and $C_{p,\mathrm{a}}$ is known. Therefore, the function $B^*_2(\omega)$ depends only on $K_{\mathrm{op,a}}$. For the other disc 'b', we get:

$$\begin{aligned} C^*_{\beta,\mathrm{b}}(\omega) &= C^*_{\mathrm{eff,b}}(\omega) B^*_2(\omega) \\ &= \frac{C^*_{\mathrm{eff,b}}(\omega)}{C^*_{\mathrm{eff,a}}(\omega)} \frac{C_{p,\mathrm{a}}}{1 - (i\omega C_{p,\mathrm{a}} / K_{\mathrm{op,a}})} \end{aligned} \tag{20}$$

Since $C^*_{\mathrm{eff,b}}(\omega)$ is measured as well, the function

$$C^*_{\beta,\mathrm{b}}(\omega) = \frac{C^*_{\mathrm{eff,b}}(\omega)}{C^*_{\mathrm{eff,a}}(\omega)} \frac{C_{p,\mathrm{a}}}{1-(i\omega C_{p,\mathrm{a}}/K_{\mathrm{op,a}})} \tag{21}$$

depends on $K_{\mathrm{op,a}}$ only. On the other hand sample 'b' is assumed a *RC*-element (Eq. (16)):

$$C^*_{\beta,\mathrm{b}}(\omega)B^*_2(\omega) = \frac{C_{p,\mathrm{b}}}{1-(i\omega C_{p,\mathrm{b}}/K_{\mathrm{op,b}})} \tag{22}$$

This means that in a Polar plot in complex plane (Cole–Cole plot) the position of the points $\mathrm{Re}(C^*_{\beta,\mathrm{b}}(\omega)$ and $\mathrm{Im}(C^*_{\beta,\mathrm{b}}(\omega))$ calculated with Eq. (22), depending on frequency ω and thermal contact $K_{\mathrm{op,b}}$, lie on a semicircle with a radius which is 1/2 of $C_{p,\mathrm{b}}$, (see Fig. 2), where $C_{p,\mathrm{b}}$ is the known heat capacity of sample disc 'b'. The same $C^*_{\beta,\mathrm{b}}(\omega)$ is described with Eq. (21), in other words, even this function—which contains measured and known quantities beside the unknown $K_{\mathrm{op,a}}$—should be a semicircle too. What must be done is to vary $K_{\mathrm{op,a}}$ until we get a semicircle in the Cole–Cole plot (Fig. 10). Here the advantage of the Cole–Cole plot becomes obvious. After $K_{\mathrm{op,a}}$ has been determined this way we are able to determine $B^*_2(\omega)$ using Eq. (19) which contains only known quantities now.

The concept of Eq. (18) requires that $B^*_2(\omega)$ should not depend on the measured particular sample and its thermal properties. This has been proved in the case of a PerkinElmer instruments Pyris-1 DSC by measuring different aluminum discs with masses ranging from 16 to 155 mg and K_{op} ranging from 20 (dry thermal contact) to 80 mW K^{-1} (wetted with silicon oil). $B^*_2(\omega)$ was found to be independent on the sample in question (within the limit of experimental uncertainties). In Fig. 3, these measurements are presented, the solid line represents the reciprocal of $B^*_2(\omega)$, the transfer function of the DSC without sample. It is almost the same for all Al discs of the measured series. Subtracting the instrument curve (solid line) from the measured curves (symbols) results in the transfer functions of the samples which are plotted in Fig. 4 (symbols) together with the fit functions (solid lines) to prove the validity of Eq. (16). The fit parameter is $\tau = C_p/K_{\mathrm{op}}$ with always the same K_{op} but different heat capacities of the respective Al discs.

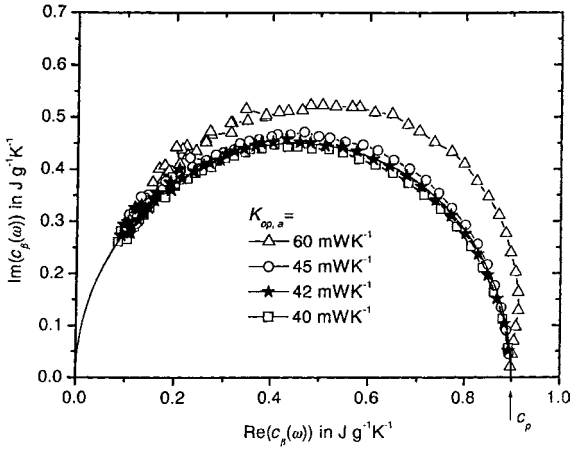

Fig. 10. Cole–Cole plot of calculated values of $C^*_{\beta,\mathrm{b}}(\omega)$ for different thermal contacts. The true values must lie on a half circle. This gives the best value: $K_{\mathrm{op,a}} = 42$ mW K^{-1} (sample 'a' and 'b': Al discs of 155 and 77 mg, respectively). PerkinElmer Instruments Pyris-1 DSC.

The apparatus calibration function $B^*_2(\omega)$ got this way should even be the same for samples with a very different heat conductivity (as polymers). This has not been proved in detail yet, but first experiments support this assumption. It should be mentioned that the method allows to determine thermal conductivity of polymer samples correctly [26], this supports the correctness of the assumptions.

We have determined $B^*_2(\omega)$ for DSCs of different type (available in our lab) using the presented algorithm. For calculations, we used whenever possible the measured temperature instead of the program temperature. All software filtering was turned off if possible. The measured heat flow rate was always zeroline corrected. The magnitude and phase angle of the reciprocal $B^*_2(\omega)$, i.e. the transfer function of the respective apparatus, are shown in Fig. 11. It is interesting to recognize, that the Pyris-1 DSC has a faster response than the DSC-2, though both calorimeters have basically the same measuring head. The reason for that is, that the DSC-2 cannot measure the sample temperature, so one has to use the program temperature for evaluation. Obviously, using the sample temperature makes the TMDSC faster. Therefore, the user is encouraged to use the sample temperature rather than the program temperature whenever possible. From Fig. 11 follows, that all types of DSC behave like a low-pass filter, i.e. the higher the frequency, the larger the "damping" of the heat flow rate and the larger the correction.

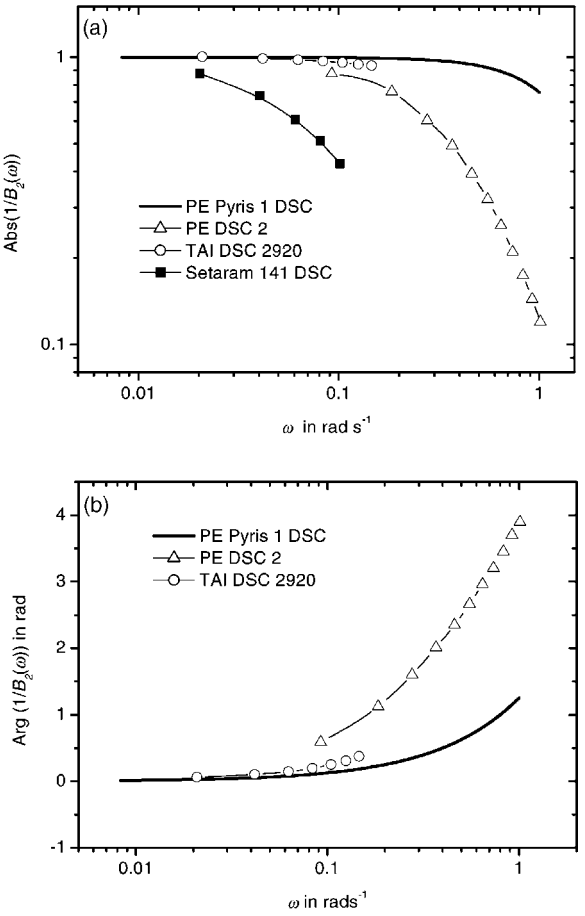

Fig. 11. Magnitude (a, Bode plot) and phase angle (b) of apparatus transfer function ($1/B_2(\omega)$) for different DSC calorimeters, determined at a temperature of about 50 °C. The particular position of the respective curve may depend on block temperature, measuring temperature and the direction of the temperature steps (heating or cooling).

With the measured $C^*_{\mathrm{eff}}(\omega)$ and the known apparatus calibration function $B^*_2(\omega)$ we are able to determine the true (apparent) heat capacity of the sample using Eqs. (16) and (18). The only parameter we have to know is K_{op}, i.e. the thermal contact between DSC and the sample in question. For a certain moment (or temperature) during the run, this quantity can be considered as independent of frequency for a given sample, consequently it can be determined from the measured quantities at different frequencies by proper evaluation. Of course the thermal contact may change during a run, especially in the transition region, but the multi-frequency measuring methods enable such an evaluation for every moment or temperature if needed [2].

To sum up, the advantage of this somewhat laborious method comes from the possibility to distinguish between the sample influence and the apparatus influence on the measured quantity and correct it separately. This allows to get more insight in material properties (as thermal conductivity) and control both the apparatus and the sample concerning its thermal transfer behavior. It should be mentioned that one can use any method of heat capacity determination with TMDSC, single as well as multi-frequency methods, to get the functions $C^*_{\mathrm{eff}}(\omega)$ which then has to be corrected to yield the apparent (complex) heat capacity of the sample.

4. Conclusions

After giving an overview of the fundamentals of heat transfer in a TMDSC and the tools of linear response theory, we have presented a number of methods for calibration of the complex heat capacity. Calibration means in this sense to determine the (complex) function which corrects for the influence of the heat transfer within the TMDSC and to the sample and to multiply the effective heat capacity measured in the TMDSC with that correction function in frequency domain. It was shown that the (reciprocal) transfer function is a suitable correction function. We can get the real transfer function of the DSC with the methods of linear response used in transfer theory. A rather easy and successful method is to measure the step response signal of the DSC (including the sample), which after Fourier transform and normalization, yields the transfer function of the measuring setup and thus the correction function for the measured heat flow rate (or heat capacity) in dependence on frequency. With a more advanced method the transfer function of the apparatus alone (without sample) can be determined and the influence of the sample can be studied separately. With multi-step procedures, it is possible to determine the transfer function at every moment of the run. This allows to calibrate the TMDSC for all temperatures or even during transitions using proper interpolation procedures. How to do that in practice of the different calibration procedures will be presented

in the second part of this paper [2]. However, certainty and reproducibility of the results should be tested carefully in every case. This is in particular true if the transfer function of the apparatus is determined separately and one wants to use it for correction of the measurements with very different types of samples (e.g. sapphire, metal and polymers). In this case it is absolute necessary to verify that the determined transfer function of the TMDSC is surely not influenced by the sample in question.

Acknowledgements

This research was supported by the German Science Foundation (Grant DFG Schi-331/5-1).

References

[1] S.M. Sarge, W. Hemminger, E. Gmelin, G.W.H. Höhne, H.K. Cammenga, W. Eysel, J. Therm. Anal. 49 (1997) 1125–1134.
[2] M. Merzlyakov, G.W.H. Höhne, C. Schick, Calibration of Magnitude and Phase of TMDSC. Thermochim. Acta 391 (2002) 69–80.
[3] F.W. Wilburn, J.R. Hesford, J.R. Flower, Anal. Chem. 40 (1968) 777–788.
[4] G.W.H. Höhne, J.E.K. Schawe, Thermochim. Acta 229 (1993) 27–36.
[5] J.E.K. Schawe, C. Schick, G.W.H. Höhne, Thermochim. Acta 229 (1993) 37–52.
[6] G.W.H. Höhne, Thermochim. Acta 69 (1983) 175–197.
[7] G.W.H. Höhne, W. Hemminger, H.J. Flammersheim, Differential Scanning Calorimetry, Springer, Berlin, 1996.
[8] G.W.H. Höhne, Thermochim. Acta 330 (1999) 45–54.
[9] T. Ozawa, K. Kanari, Thermochim. Acta 288 (1996) 39–51.
[10] T. Ozawa, K. Kanari, J. Thermal Anal. 54 (1998) 521–534.
[11] I. Hatta, N. Katayama, J. Thermal Anal. 54 (1998) 577–584.
[12] S.X. Xu, Y. Li, Y.P. Feng, Thermochim. Acta 360 (2000) 157–168.
[13] H. Hoff, Thermochim. Acta 187 (1991) 293–307.
[14] J.E.K. Schawe, W. Winter, Thermochim. Acta 298 (1997) 9–16.
[15] A.A. Lacey, C. Nikolopoulos, M. Reading, J. Thermal Anal. 50 (1997) 279–333.
[16] G.W.H. Höhne, N.B. Shenogina, Thermochim. Acta 310 (1998) 47–51.
[17] B. Schenker, F. Stäger, Thermochim. Acta 304/305 (1997) 219–228.
[18] F.U. Buehler, C.J. Martin, J.C. Seferis, J. Thermal Anal. 54 (1998) 501–519.
[19] F.U. Buehler, J.C. Seferis, Thermochim. Acta 334 (1999) 49–55.
[20] I. Hatta, A.A. Minakov, Thermochim. Acta 330 (1999) 39–44.
[21] R. Androsch, B. Wunderlich, Thermochim. Acta 333 (1999) 27–32.
[22] R. Androsch, I. Moon, S. Kreitmeier, B. Wunderlich, Thermochim. Acta 357 (2000) 267–278.
[23] A. Toda, T. Arita, C. Tomita, M. Hikosaka, Polymer 41 (2000) 8941–8951.
[24] I. Hatta, S. Muramatsu, Jpn. J. Appl. Phys. 35 (1996) 858–860.
[25] M. Merzlyakov, C. Schick, Thermochim. Acta 330 (1999) 65–73.
[26] M. Merzlyakov, C. Schick, Thermochim. Acta 377 (2001) 183–191.